

Tandem Förster Resonance Energy Transfer Induced Luminescent Ratiometric Thermometry in Dye-Encapsulated Biological Metal–Organic Frameworks

Hong Cai, Weigang Lu, Chen Yang, Ming Zhang, Mian Li, Chi-Ming Che, and Dan Li*

Luminescent ratiometric thermometers (LRTs) based on the emission intensity ratio with self-reference functions guarantee a temperature sensing of fast response, high precision, and excellent spatial resolution. For monitoring temperature at the cellular level, the use of metal–organic frameworks (MOFs) as probes, especially biocompatible ones, is still in its nascency. By employing a biological MOF, $Zn_3(\text{benzene-1,3,5-tricarboxyl})_2(\text{adenine})(\text{H}_2\text{O})$ (ZnBTCA), as a host and thermosensitive fluorescent dyes as guests, a series of dye@ZnBTCA is synthesized and studied as potential LRT materials, featuring a unique mechanism of tandem Förster resonance energy transfer among the MOF host and the multiple dye guests. This scenario is significantly different from the commonly reported lanthanide or mixed-lanthanide MOFs where energy transfer occurs between lanthanide ions. Acf-RB@ZnBTCA, in particular, not only exhibits highly efficient ratiometric temperature-sensing properties under physiological cellular conditions but also can be excited under visible light.

As opposed to conventional thermometry, which often requires direct contact between the probe and the target, optical thermometry has recently attracted increasing attention because of advantages such as noninvasive, accurate, large-scale imaging, and capable of working even in strong electromagnetic fields.^[1] Among a variety of optical methods utilized for thermometry, including thermal reflection, Rayleigh scattering, Raman

scattering, etc., the one based on luminescence possesses the merits of fast response, excellent spatial resolution, and high sensitivity, which translate into great advantages for microfluidic and bio-imaging applications.^[2] Particularly, by employing the intensity ratio of two independent emissions in the same materials, luminescent ratiometric thermometers (LRTs) are independent of sensor concentration, excitation power, and drifts of the optoelectronic systems. These unique characteristics ensure accurate and reliable temperature sensing.^[3] On the other hand, temperature is a crucial parameter for monitoring protoplast events in order to track the cellular pathology and physiology as well as understand the treatments and diagnoses. Hence, the development of biocompatible temperature probes is

highly desired. Various types of material-based thermometers have been developed for monitoring temperature at the cellular level, including europium (III) complexes, nanomaterials, polymers, quantum dots, and biomaterial microcantilevers.^[4,5]


Metal–organic frameworks (MOFs) are one of the most promising thermochromic materials due to their remarkable structural diversities and tunable luminescent properties. Light-emitting species such as metal ions and organic ligands can be periodically integrated into the framework; this unique characteristic along with high porosity effectively prevent aggregation-induced luminescence quenching and make MOF materials excellent candidates for encapsulating other luminescent species. For example, lanthanide ions, luminescent dyes, and quantum dots could be encapsulated in MOFs for applications in color control and temperature sensing.^[4d,e,f,9b] Many cases of LRT-MOFs based on lanthanide ions have received much attention for their interesting temperature-dependent luminescence properties.^[3a,4b,5b,6,7] More recently, LRT-MOFs constructed with mixed lanthanide ions (usually Tb^{3+} and Eu^{3+}) have been reported by Qian and Chen et al. with improved sensing performance and sensitivity.^[1b,c,3a,4b,7] However, scarcity of rare earth metals could limit their extensive applications of any kind. Therefore, it is equally challenging to explore LRT-MOFs constructed with readily available and inexpensive metals in this line of work. For monitoring temperature at the cellular level, exploring LRT-MOFs with biocompatibility, although still in its nascency, is of great significance.

Dr. H. Cai
School of Chemistry and Environmental Engineering
Hanshan Normal University
Chaozhou, Guangdong 521041, P. R. China

Dr. H. Cai, M. Zhang, M. Li
Department of Chemistry
Shantou University
Guangdong 515063, P. R. China

Prof. W. Lu, Prof. D. Li
College of Chemistry and Materials Science
Jinan University
Guangzhou, Guangdong 510632, P. R. China
E-mail: danli@jnu.edu.cn

Dr. C. Yang, M. Zhang, Prof. C.-M. Che
State Key Laboratory of Synthetic Chemistry
and Department of Chemistry
The University of Hong Kong
Pokfulam Road, Hong Kong 999077, P. R. China

 The ORCID identification number(s) for the author(s) of this article can be found under <https://doi.org/10.1002/adom.201801149>.

DOI: 10.1002/adom.201801149

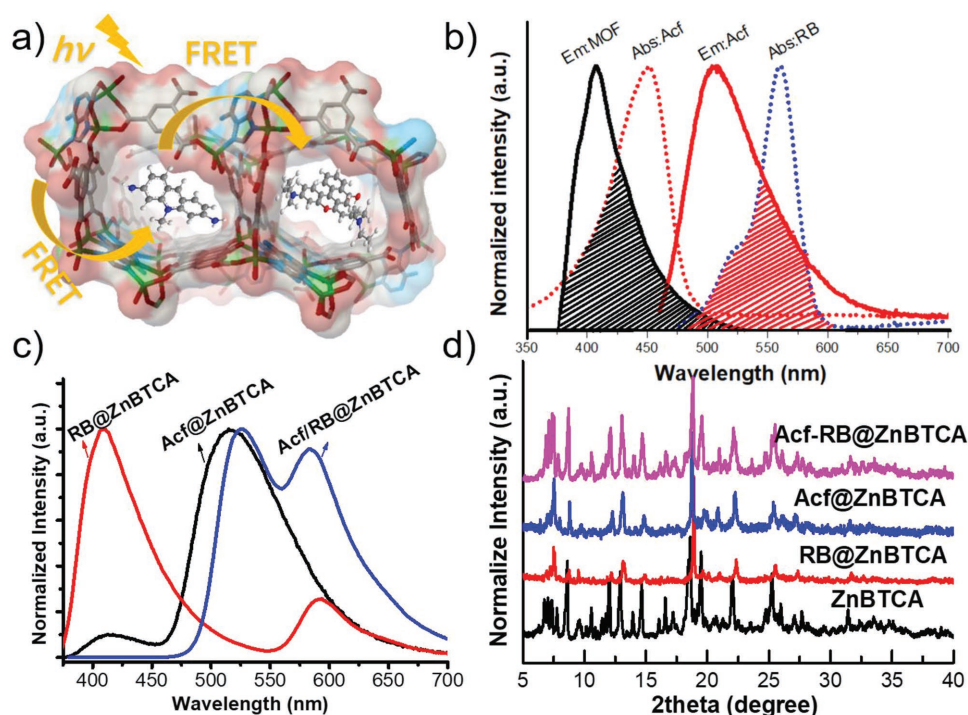


Figure 1. a) Illustration of tandem FRET pathway in a mixed-dye@ZnBTCA system. b) Black shaded area is the overlap of emission spectrum of ZnBTCA (black solid line) and absorbance spectrum of Acf (red dotted line), the red shaded area is the overlap of emission spectrum of Acf (red solid line) and absorbance spectrum of RB (blue dotted line). c) Emission spectra of Acf@ZnBTCA (black), RB@ZnBTCA (red), and Acf-RB@ZnBTCA (blue) at room temperature. d) PXRD patterns of ZnBTCA, RB@ZnBTCA, Acf@ZnBTCA, and Acf-RB@ZnBTCA.

Mixed-lanthanide MOFs, especially those Tb_xEu_y -MOFs, demonstrated a temperature-dependent luminescence behavior and, more importantly, the luminescent intensity ratio of Tb^{3+} and Eu^{3+} ions is linearly correlated with temperature in a certain range.^[1c,7] This unique property was attributed to the energy transfer between the two light-emitting metal ions. It is known that luminophores capable of energy transfer are not limited to lanthanides, which inspired us to design and investigate lanthanide-free MOFs as novel LRTs via a host-guest dual-emission strategy.^[8] In further consideration of biological applications, an adenine-based MOF, $Zn_3(\text{benzene-1,3,5-tricarboxyl})_2(\text{adenine})(H_2O)$ (ZnBTCA), was selected as donor platform due to its excellent biocompatibility^[9a,c,d,e,10] (Figure 1a). ZnBTCA possesses sinusoidal-like nanochannel with Watson–Crick open sites toward the pores, which are prone to form H-bond for DNA-stains.^[9a,b] Thermosensitive luminescent dyes were chosen as the guests to integrate with ZnBTCA, and the system was named as dye@ZnBTCA. The spectral overlap between ZnBTCA and dye is a requisite for Förster resonance energy transfer (FRET, Figure 1b), which dictates the emission of dye is photosensitized by ZnBTCA through energy transfer from donor ZnBTCA to acceptor dye. Consequently, the emission intensity of dye increases at the expense of the emission intensity of ZnBTCA. Owing to their thermosensitivity, the luminescent intensity ratio of host/guest (ZnBTCA/dye) responds to the surrounding temperature. Additionally, the emission intensity of dye can be used as an internal reference, rendering dye@ZnBTCA a self-calibrating temperature sensor.

The common biological stain acriflavine (Acf) shows temperature-sensitive luminescence.^[11] An overlap was observed between the absorption spectrum of Acf and the emission spectrum of ZnBTCA (Figure 1b), which satisfies the primary requirement for achieving efficient FRET from ZnBTCA to Acf. Thus, Acf was selected as the guest molecule and encapsulated into ZnBTCA, and the system was labeled as Acf@ZnBTCA. The samples were sonicated and filtered to get rid of the residual Acf on the surface of crystals, and then immersed in *N,N*-dimethylformamide (DMF) for 24 h. No leakage of Acf from Acf@ZnBTCA was detected as evidenced by UV–vis spectra of the residual DMF solution (Figures S2 and S3, Supporting Information). We surmise that the encapsulation of Acf is not simply diffusion controlled and there is a strong dipole–dipole interaction between amino groups in Acf molecule and open Watson–Crick sites as well as carboxyl-O sites within ZnBTCA framework.^[9a] Thermogravimetric analysis showed that the thermal decomposition of Acf was at 300 °C, compared with Acf@ZnBTCA at 400 °C, which suggested that Acf molecules were indeed encapsulated into ZnBTCA and decomposition was avoided (Figure S4, Supporting Information). The crystallinity of Acf@ZnBTCA was confirmed by its powder X-ray diffraction (PXRD) pattern (Figure 1d), which was in good agreement with that of the as-synthesized ZnBTCA, indicating the intactness of the framework after encapsulation.

The strong dipole–dipole interaction is an important factor to realizing FRET. To further determine the existence of such an interaction between Acf molecule and the MOF matrix, emission spectra of Acf@ZnBTCA were collected in the

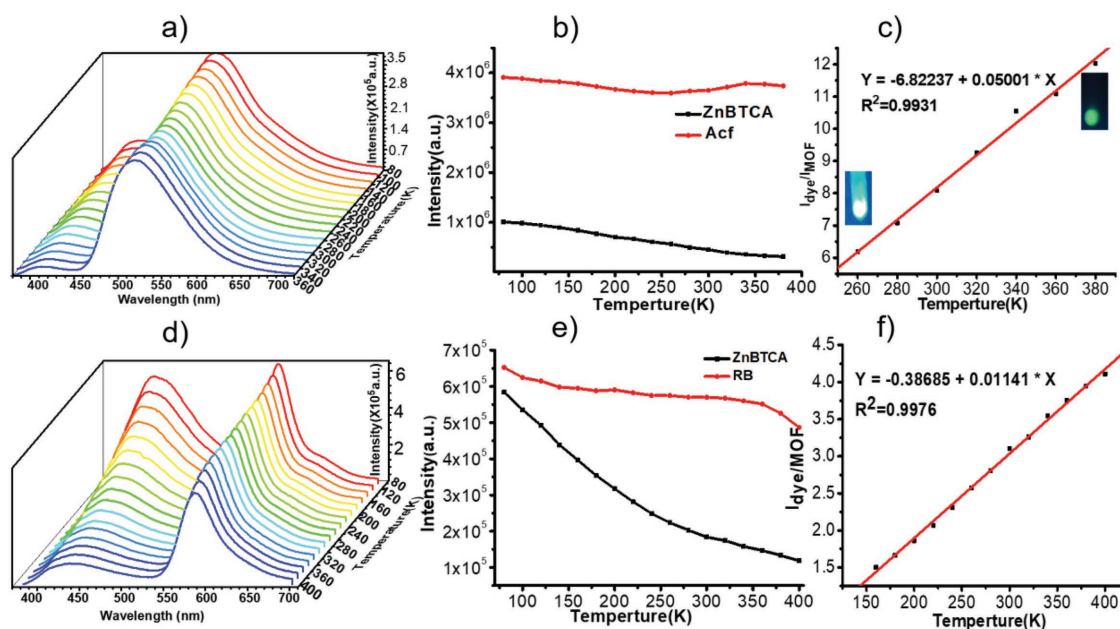


Figure 2. a) Solid state luminescent spectra of Acf@ZnBTCA excited at 340 nm at different temperatures. b) Emission intensity of Acf and ZnBTCA in an Acf@ZnBTCA system plotted against temperature. c) Temperature dependence of emission intensity ratio of $I_{\text{Acf}}/I_{\text{MOF}}$ in the range of 260–380 K. d) Solid state luminescent spectra of RB@ZnBTCA excited at 340 nm at different temperatures. e) Emission intensity of RB and ZnBTCA in an RB@ZnBTCA system plotted against temperature. f) Temperature dependence of emission intensity ratio of $I_{\text{RB}}/I_{\text{MOF}}$ in the range of 160–400 K.

solid state at different temperatures (Figure 2a). As expected, Acf@ZnBTCA displayed the characteristic emissions of both Acf ($\lambda_{\text{em}}^{\text{max}} \approx 500$ nm) and ZnBTCA ($\lambda_{\text{em}}^{\text{max}} \approx 410$ nm) upon excitation at 340 nm. From 80 to 260 K, Acf showed little sensitivity to temperature since the emission intensity (I_{dye}) barely changed, yet it began to increase when the temperature exceeded 280 K (Figure 2b, red line). The emission intensity of ZnBTCA (I_{MOF}), on the other hand, continuously decreased throughout the entire temperature range from 80 to 380 K (Figure 2b, black line). Remarkably, the different variation in the emission intensity of ZnBTCA and Acf renders the $I_{\text{dye}}/I_{\text{MOF}}$ ratio to be linearly correlated with temperature in the range of 260–380 K. The temperature can be expressed in terms of $I_{\text{dye}}/I_{\text{MOF}}$ as in Equation (1)

$$T = 136.42 + 19.996 \frac{I_{\text{dye}}}{I_{\text{MOF}}} \quad (1)$$

As illustrated in Figure 2c and Figure S5b in the Supporting Information, the maximum relative sensitivity (S_r) of Acf@ZnBTCA was determined to be $5.001\% \text{ K}^{-1}$, and the emission color changed from cyan at 280 K to green at 380 K (Figure S5b, Supporting Information). It was worth mentioning that the emission maximum of ZnBTCA in Acf@ZnBTCA blueshifted from 423 to 410 nm, whereas Acf redshifted from 500 to 505 nm as temperature increased (Figure S5a, Supporting Information). The slightly spectral shifts might result from the strong dipole–dipole interactions between host framework and guest dye, which probably involve a certain degree of electron transfer.

The energy transfer efficiencies (Φ_{ET}) calculated from the emission lifetimes of the guest and the host are listed in Table 1.^[8] The lifetime of pristine ZnBTCA (τ_{MOF}) was

determined to be 9.79 ns, while it ($\tau_{\text{MOF-Acf}}$) was 7.21 ns in the Acf@ZnBTCA system. Similar to the situation of the heterogeneity interaction between Acf and DNA, the amino groups in Acf may interact with ZnBTCA bearing open Watson–Crick sites.^[9a] The strong dipole–dipole interaction, the overlapped spectrum, and the host–guest confinement—a synergy of all these factors—made the lifetime of ZnBTCA decreased, resulting in energy transfer from ZnBTCA to Acf. Φ_{ET} can be estimated to be around 26.3% at room temperature.

The fluorescence time-resolve emission analysis of Acf@ZnBTCA was carried out at 77 K and room temperature, respectively (Figure S6, Supporting Information). At 77 K particularly (Figure S6b, Supporting Information), the emission intensity of host framework and guest dye were almost the same in the beginning, but both quickly decreased after 4 ns, and eventually, the intensity of Acf was considerably higher than ZnBTCA after 10 ns. All these data suggested that the energy did transfer from ZnBTCA to Acf in the process, resulting in a significant boost of $I_{\text{dye}}/I_{\text{MOF}}$ ratio. In other words, the S_r was endorsed through an FRET pathway.

As shown in Table S1 in the Supporting Information, the percentage of Acf in Acf@ZnBTCA could influence the temperature sensitivity, resulting in S_r values ranging from 0.16% (0.02 wt% of Acf) to $5.001\% \text{ K}^{-1}$ (0.2 wt% of Acf). Compared with mixed-lanthanide MOFs (Table S2, Supporting Information), Acf@ZnBTCA showed higher S_r values in the range of 260–380 K. Furthermore, its stability was confirmed by three cycles of measurements showing almost no loss of sensitivity (Figure S7a, Supporting Information). Considering the biocompatibility and availability of zinc metal, it is sufficient to conclude that Acf@ZnBTCA has its own advantages in many aspects and is an excellent LRT candidate material.

Table 1. Lifetime of ZnBTCA and dye@ZnBTCA system as well as energy transfer efficiency calculation.

Type ^{a)}	Lifetime of ZnBTCA [ns]	Lifetime of dye [ns]	Energy transfer efficiency (Φ_{ET}) [%]
ZnBTCA	9.79/11.482 ^{b)}	N/A ^{c)}	N/A
Acf@ZnBTCA	7.21/7.27 ^{b)}	7.62/9.64 ^{b)}	26.3%/36.7% ^{b)}
RB@ZnBTCA	10.36	11.57	N/A
Acf-RB@ZnBTCA	3.95	6.88 ^{d)} /12.28 ^{e)}	59.7% ^{f)} /9.7% ^{g)}

^{a)}Determined at room temperature; ^{b)}Determined at 77 K; ^{c)}N/A stands for not applicable; ^{d)}Lifetime of Acf in Acf-RB@ZnBTCA system; ^{e)}Lifetime of RB in Acf-RB@ZnBTCA system; ^{f)} Φ_{ET} from ZnBTCA to Acf, ^{g)} Φ_{ET} from Acf to RB.

Rhodamine B (RB) and its derivatives are well known for their fluorescence sensitivity to temperature.^[12] Although cationic RB belongs to the oversized group relative to the pore size of ZnBTCA,^[9a] it can also be moderately adsorbed by anionic ZnBTCA through electrostatic interaction as well as uptake into the mesopores of crystal defects. Therefore we chose to study RB@ZnBTCA as a control, for which we expected no FRET phenomena observed because the absorption spectrum of RB barely overlapped with the emission spectrum of ZnBTCA (Figure 1b), and the host–guest confinement is absence due to surface adsorption.

As expected, the emission peaks of ZnBTCA and RB showed no obvious shifts in the RB@ZnBTCA system at different temperatures (Figure 2d and Figure S8, Supporting Information). Influenced by surface attachment of RB, the lifetime of RB@ZnBTCA was about 10.48 ns, which was slightly longer than the pristine one, indicating an absence of FRET (Table 1). Furthermore, the fluorescence intensities of both ZnBTCA and RB continuously decreased as temperature increased (Figure 2e). To take a closer look, the I_{dye} of RB decreased slowly at cryogenic temperature, then rather quickly when the temperature reached 320 K; whereas the I_{MOF} of ZnBTCA showed a different response in the same temperature range, decreasing rather quickly from 80 to 320 K and then slowly from 320 to 400 K. The drop of luminescence intensities for both RB and ZnBTCA is commonly attributed to their thermal quenching behaviors.^[12] As shown in the Figure 2f, the I_{dye}/I_{MOF} ratio of the RB@ZnBTCA system showed linear relationship within the temperature range of 150–400 K (Equation (2)).

$$T = 33.90 + 87.64 \frac{I_{dye}}{I_{MOF}} \quad (2)$$

Increasing the content of RB could also enhance the luminescence sensitivity for RB@ZnBTCA, the maximum S_r was calculated to be 1.141% K⁻¹ (Figure S8, Supporting Information), which is lower than that of Acf@ZnBTCA possibly due to the absence of FRET in the former system. The stability of RB@ZnBTCA was confirmed by three cycles of measurement without showing notable loss of sensitivity to temperature (Figure S7b, Supporting Information).

The above comparison between the different temperature sensing behaviors of Acf@ZnBTCA and RB@ZnBTCA confirms FRET is the working mechanism for boosting the sensitivity (S_r) of the LRTs investigated. From the overlapped spectra (Figure 1b), we noticed that the absorption spectrum of RB and the emission spectrum of Acf are largely overlapped. Therefore

we propose a new working mechanism, i.e., tandem FRET, that is, the energy first transfers from ZnBTCA to Acf and then from Acf to RB. An attempt was made to incorporate both Acf and RB with ZnBTCA (denoted as Acf-RB@ZnBTCA) and its performance as LRT probe was examined (Figure S11 and Scheme S1, Supporting Information).

It was then found that the I_{Acf}/I_{RB} was linearly correlated within the temperature range of 270–340 K, and the S_r of Acf-RB@ZnBTCA was calculated to be 0.713% K⁻¹. The emission peaks of both Acf and RB gradually redshifted as temperature increased. The lifetime of host was 3.95 ns, significantly shorter than the pristine ZnBTCA, indicating more efficient energy transfer compared with the above two systems, while the lifetimes of Acf and RB were 6.88 and 12.28 ns, respectively. The decrease in the lifetime of the host was accompanied by an increase in the lifetime of dyes owing to a tandem FRET pathway, in which the energy transfer initially from ZnBTCA to Acf and then to RB, with Φ_{ET} values of 59.7% and 9.7%, respectively (Table 1). The energy transfer efficiency is much higher for the former process. Given that the extent of spectral overlapping is comparable for the two processes (cf. black and red shadow regions in Figure 1b), the different Φ_{ET} values are likely due to the lack of host–guest confinement for the Acf-to-RB FRET process, which is distance dependent.

There are three types of cavities interconnected in ZnBTCA, resulting in the formation of 1D channels with large opening windows ($11 \times 8 \text{ \AA}^2$).^[9a] The inside channel view of ZnBTCA integrated with the Connolly surface was shown in Figure S9 in the Supporting Information. The xyz dimensions of Acf and RB molecules are $10.50 \times 5.04 \times 3.79 \text{ \AA}^3$ and $14.90 \times 11.82 \times 5.00 \text{ \AA}^3$, respectively (Figure S10, Supporting Information). Therefore, Acf molecules could be completely encapsulated into the channel of ZnBTCA. In comparison, the oversized RB could be adsorbed on the surface of ZnBTCA through electrostatic interaction as well as into the mesopores of crystal defects. Scanning electron microscopy (SEM) images showed the surface topography of ZnBTCA, Acf@ZnBTCA, and RB@ZnBTCA (Figure 3). It could be clearly seen that the crystals contain a lot of mesopores.

The fact that this mixed-dye Acf-RB@ZnBTCA system can be excited by 410 nm visible-light, rendering its potential biological applications under the visible light irradiation, which is of great practical importance. Thus, the results present a new direction for the rational design of biocompatible and lanthanide-free LRT materials.

Recent medical studies suggest that some cancer cells are at an elevated temperature compared to normal cells because

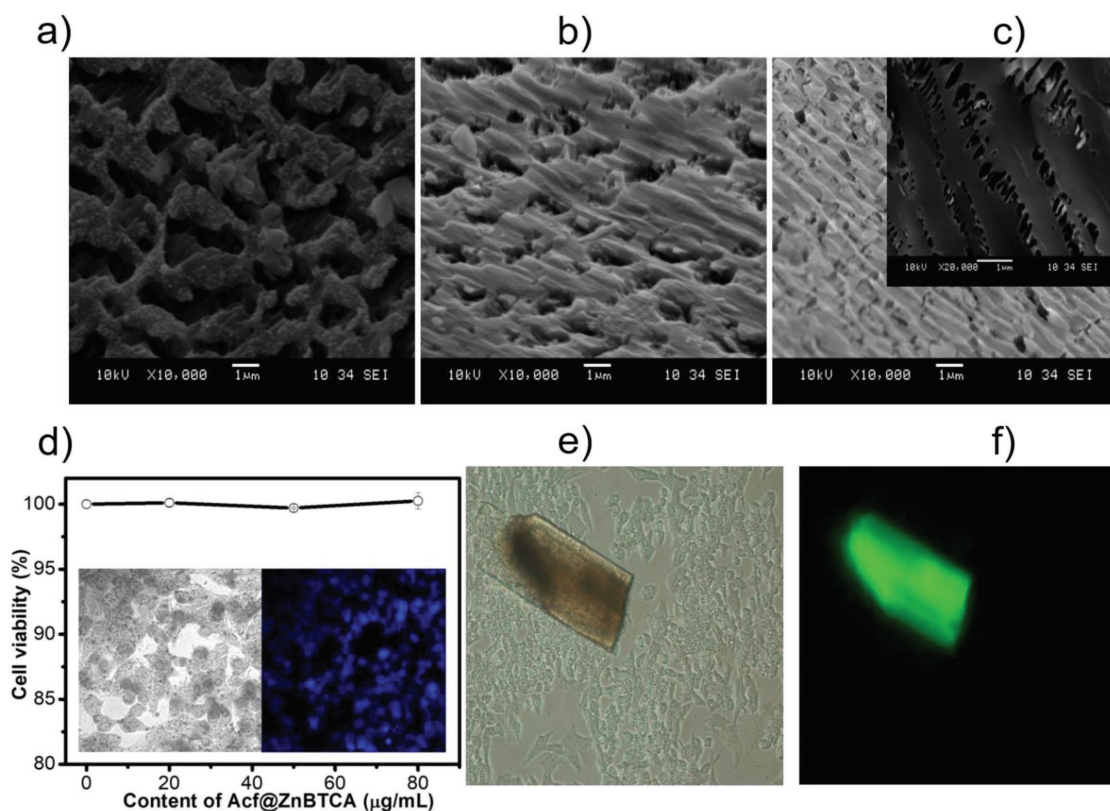


Figure 3. a) SEM image of ZnBTCA. b) SEM image of Acf@ZnBTCA. c) SEM image of RB@ZnBTCA, inset: 20 000× magnification. d) Cell viability versus content of Acf@ZnBTCA, obtained from cultured MiHA cells with the untreated cells as a control, inset: confocal laser scanning microscope images of living MiHA cells in the bright and dark fields. e, f) Fluorescent inverted microscope images of living MiHA cells after 48 h exposure to Acf@ZnBTCA at 80 μg mL⁻¹ at bright and dark images.

of their extraordinary metabolic rates.^[13] Therefore, real-time temperature tracking in biological systems featuring high spatial resolution is extremely important, especially within the range of 0–70 °C. Considering such applications, ZnBTCA displayed a very good biocompatibility, showing no cytotoxicity toward normal Madin–Darby canine kidney (MDCK) epithelial cells in vitro assays.^[9c,d] As a preliminary test, cytotoxicity studies of Acf@ZnBTCA were carried out by MTT assay [MTT = 3-(4,5-dimethylthiazol-2-yl)-2,5-diphenyltetrazolium bromide] using normal human hepatocytes cells (MiHA). After exposed to Acf@ZnBTCA for 48 h, MiHA cell viability maintained above 99% even when the Acf@ZnBTCA concentration was raised to 80 μg mL⁻¹ (Figure 3d). Fluorescent inverted microscope images of living MiHA cells were collected after exposed to Acf@ZnBTCA for 48 h, showing the vast majority of cells were survived (Figure 3e,f).

Moreover, ZnBTCA, Acf@ZnBTCA, and RB@ZnBTCA were added into MDCK^[9c] and the surviving cells were again clearly observed at both 4 °C and room temperature as evidenced by the fluorescent inverted microscope images (Figures S12–S14, Supporting Information), indicating that Acf@ZnBTCA barely damaged the MDCK cells. To examine the effect of Acf@ZnBTCA on nuclear DNA, imaging of cells was carried out using 4',6-diamidino-2-phenylindole (DAPI) staining for 5 min on a confocal laser scanning microscope. As shown in Figure 3d inset, the retaining of blue fluorescence

suggested that Acf@ZnBTCA did not incur any noticeable damage to the nuclear DNA either. These results demonstrated that the Acf@ZnBTCA is of low cytotoxicity, which is highly desired for thermometry at the cellular level in vitro.

In order to explore the probability of visible light excitation, Acf-RB@ZnBTCA (80 μg mL⁻¹) was added in the living MDCK cells for 48 h and then irradiated at 450 and 510 nm respectively at 4 °C and room temperature. The fluorescent inverted microscope images (Figure S15, Supporting Information) showed that the change in emission color was subtle and might not be visible to the naked eye, but the intensity was clearly diminished as temperature increased. It is a significant step forward in the design of LRT materials for cellular temperature monitoring in terms of biocompatibility and visible light excitation.

In conclusion, thermosensitive fluorescent dyes were encapsulated into the biocompatible ZnBTCA to afford dual-emitting dye@ZnBTCA, which were demonstrated as highly sensitive and stable LRT materials. Particularly, the $I_{\text{dye}}/I_{\text{MOF}}$ of Acf@ZnBTCA system responded linearly to temperature within a wide range of 260–380 K, and the maximum S_T could reach up to 5.001% K⁻¹. Although there are other types of LRT materials,^[1a,4d,e,14] including one based on polymer nanoparticle showing a record S_T of 15.4% K⁻¹,^[4c] the present Acf@ZnBTCA LRT is among the highest-value sensitivity for MOF-based LRT. Moreover, as a proof of concept of tandem FRET process, a mixed-dye Acf-RB@ZnBTCA system was realized, featuring a

unique working mechanism and visible-light excitation. Preliminary biological evaluations, including biocompatibility and the very low MDCK cells toxicity in vitro, were implemented, indicating these LRT materials are suitable for biological applications. Further attempts toward real application, such as surface nanocrystallization of the LRT materials to reach the cellular level, are ongoing.

Experimental Section

Preparation of Acf-RB@ZnBTCA: 10 mg of ZnBTCA was immersed in 1 mL of DMF solution containing Acf and RB (10 µg each). After allowed to stand still overnight, the solid was collected by filtration, washed with fresh DMF, denoted as Acf-RB@ZnBTCA. The contents of Acf and RB were determined by UV-vis absorption.

Supporting Information

Supporting Information is available from the Wiley Online Library or from the author.

Acknowledgements

This work was financially supported by the National Natural Science Foundation of China (21731002 and 21701038) and Scientific Research Start-up Funds of Hanshan Normal University (QD20161009).

Conflict of Interest

The authors declare no conflict of interest.

Keywords

Förster resonance energy transfer, host-guest chemistry, luminescent ratiometric thermometry, metal-organic framework

Received: August 23, 2018
Revised: September 30, 2018
Published online:

- [1] a) X. D. Wang, O. S. Wolfbeis, R. J. Meier, *Chem. Soc. Rev.* **2013**, 42, 7834; b) Y. Cui, R. Song, J. Yu, M. Liu, Z. Wang, C. Wu, Y. Yang, Z. Wang, B. Chen, G. Qian, *Adv. Mater.* **2015**, 27, 1420; c) Y. Cui, F. Zhu, B. Chen, G. Qian, *Chem. Commun.* **2015**, 51, 7420; d) Y. Zhou, D. Zhang, J. Zeng, N. Gan, J. Cuan, *Talanta* **2018**, 181, 410; e) A. M. Kaczmarek, R. Van Deun, M. K. Kaczmarek, *Sens. Actuators, B* **2018**, 273, 696.
- [2] a) B. d. Rosal, E. Ximendes, U. Rocha, D. Jaque, *Adv. Opt. Mater.* **2017**, 5, 1600508; b) B. Dong, B. Cao, Y. He, Z. Liu, Z. Li, Z. Feng,

- Adv. Mater.* **2012**, 24, 1987; c) J. Qiao, X. Mu, L. Qi, *Biosens. Bioelectron.* **2016**, 85, 403; d) M. Nakano, T. Nagai, *J. Photochem. Photobiol., C* **2017**, 30, 2.
- [3] a) T. Xia, Y. Cui, Y. Yang, G. Qian, *J. Mater. Chem. C* **2017**, 5, 5044; b) J. Wang, M. Li, J. Zheng, X. Huang, D. Li, *Chem. Commun.* **2014**, 50, 9115; c) D. Yue, Y. Huang, L. Zhang, K. Jiang, X. Zhang, Y. Cui, Y. Yu, G. Qian, *J. Mater. Chem. C* **2018**, 6, 2054; d) D. Yang, D. Liu, C. Tian, S. Wang, H. Li, *J. Colloid Interface Sci.* **2018**, 519, 11.
- [4] a) Ž. Antić, M. D. Dramićanin, K. Prashanthi, D. Jovanović, S. Kuzman, T. Thundat, *Adv. Mater.* **2016**, 28, 7745; b) T. Xia, T. Song, Y. Cui, Y. Yang, G. Qian, *Dalton Trans.* **2016**, 45, 18689; c) Y. Wu, J. Liu, J. Ma, Y. Liu, Y. Wang, D. Wu, *ACS Appl. Mater. Interfaces* **2016**, 8, 14396; d) C. Yao, Y. Xu, Z. Xia, *J. Mater. Chem. C* **2018**, 6, 4396; e) D. Zhang, Y. Xu, Q. Liu, Z. Xia, *Inorg. Chem.* **2018**, 57, 4613; f) Y. Zhou, B. Yan, *J. Mater. Chem. C* **2015**, 3, 9353.
- [5] a) L. Wei, Y. Ma, X. Shi, Y. Wang, X. Su, C. Yu, S. Xiang, L. Xiao, B. Chen, *J. Mater. Chem. B* **2017**, 5, 3383; b) J. Rocha, C. D. S. Brites, L. D. Carlos, *Chem. - Eur. J.* **2016**, 22, 14782; c) D. Zhao, J. Zhang, D. Yue, X. Lian, Y. Cui, Y. Yang, G. Qian, *Chem. Commun.* **2016**, 52, 8259; d) G. Huang, C. Wang, X. Xu, Y. Cui, *RSC Adv.* **2016**, 6, 58113.
- [6] a) L. Li, Y. Zhu, X. Zhou, C. D. S. Brites, D. Ananias, Z. Lin, F. A. A. Paz, J. Rocha, W. Huang, L. D. Carlos, *Adv. Funct. Mater.* **2016**, 26, 8677; b) Y. Wei, R. Sa, Q. Li, K. Wu, *Dalton Trans.* **2015**, 44, 3067; c) C. D. S. Brites, P. P. Lima, L. D. Carlos, *J. Lumin.* **2016**, 169, 497.
- [7] a) B. Chen, Y. Yang, F. Zapata, G. Lin, G. Qian, E. B. Lobkovsky, *Adv. Mater.* **2007**, 19, 1693; b) Y. Cui, H. Xu, Y. Yue, Z. Guo, J. Yu, Z. Chen, J. Gao, Y. Yang, G. Qian, B. Chen, *J. Am. Chem. Soc.* **2012**, 134, 3979; c) X. Rao, T. Song, J. Gao, Y. Cui, Y. Yang, C. Wu, B. Chen, G. Qian, *J. Am. Chem. Soc.* **2013**, 135, 15559; d) Y. Cui, W. Zou, R. Song, J. Yu, W. Zhang, Y. Yang, G. Qian, *Chem. Commun.* **2014**, 50, 719.
- [8] Q. Xiao, Y. Li, F. Li, M. Zhang, Z. Zhang, H. Lin, *Nanoscale* **2014**, 6, 10179.
- [9] a) H. Cai, M. Li, X.-R. Lin, W. Chen, G.-H. Chen, X.-C. Huang, D. Li, *Angew. Chem., Int. Ed.* **2015**, 54, 10454; b) H. Cai, L.-L. Xu, H.-Y. Lai, J.-Y. Liu, S.W. Ng, D. Li, *Chem. Commun.* **2017**, 53, 7917; c) R. W.-Y. Sun, M. Zhang, D. Li, Z.-F. Zhang, H. Cai, M. Li, Y.-J. Xian, S. W. Ng, A. S.-T. Wong, *Chem. - Eur. J.* **2015**, 21, 18534; d) R. W.-Y. Sun, M. Zhang, D. Li, M. Li, A. S.-T. Wong, *J. Inorg. Biochem.* **2016**, 163, 1; e) H. Cai, Y.-L. Huang, D. Li, *Coord. Chem. Rev.* **2018**, <https://doi.org/10.1016/j.ccr.2017.12.003>; f) R. K. Tubbs, W. E. Ditmars, Q. Van Winkle, *J. Mol. Biol.* **1964**, 9, 545.
- [10] V. R. de la Rosa, W. M. Nau, R. Hoogenboom, *Org. Biomol. Chem.* **2015**, 13, 3048.
- [11] J. C. Fister, D. Rank, J. M. Harris, *Anal. Chem.* **1995**, 67, 4269.
- [12] a) Y. Wu, J. Liu, Y. Wang, K. Li, J. Xu, D. Wu, *ACS Appl. Mater. Interfaces* **2017**, 9, 11073; b) P. Löw, B. Kim, N. Takama, C. Bergaud, *Small* **2008**, 4, 908; c) A. Ozawa, A. Shimizu, R. Nishiyabu, Y. Kubo, *Chem. Commun.* **2015**, 51, 118; d) A. Soleilhac, M. Girod, P. Dugourd, B. Burdin, J. Parvole, P.-Y. Dugas, F. Bayard, E. Lacôte, E. Bourgeat-Lami, R. Antoine, *Langmuir* **2016**, 32, 4052.
- [13] a) R. J. DeBerardinis, J. J. Lum, G. Hatzivassiliou, C. B. Thompson, *Cell Metab.* **2008**, 7, 11; b) M. Monti, L. Brandt, J. Ikomi-Kumm, H. Olsson, J. Scand, *Haematologia* **1986**, 36, 353.
- [14] a) S. Cao, J. Zheng, J. Zhao, Z. Yang, M. Shang, C. Li, W. Yang, X. Fang, *Adv. Funct. Mater.* **2016**, 26, 7224; b) S. Uchiyama, A. P. de Silva, *J. Chem. Educ.* **2006**, 83, 720; c) P. Wu, X. Hou, J. Xu, H. Chen, *Nanoscale* **2016**, 8, 8427.